

# The effect of Fe impurity on electronic and optical properties of graphene-like InAs: a DFT-based study

L Sohrabi<sup>1\*</sup>, A Boochani<sup>2</sup> and A Taghavi<sup>1</sup>

<sup>1</sup>Department of Physics, Qaemshahr Branch, Islamic Azad University, Qaemshahr, Iran

<sup>2</sup>Department of Physics, Kermanshah Branch, Islamic Azad University, Kermanshah, Iran

Received: 02 November 2020 / Accepted: 05 April 2021 / Published online: 6 May 2021

**Abstract:** The first-principles calculations have been applied to investigate the impact of Fe impurity on the electronic, magnetic, and optical properties of graphene-like InAs and compare the results. The calculations have been accomplished through the full-potential augmented plane wave technique in the density functional theory framework using WIEN2k computational software. The band structures, density of states, and magnetic moment have been calculated. Since the presence of Fe causes magnetic effects such as spin-orbit interaction and electronic treatment variations, substituting In by Fe changes the non-magnetic InAs nanosheets semiconductor to a metalloid with the magnetic moment of about 5 Bohr magneton. Moreover, both real and imaginary diagrams of the dielectric function, loss function, optical conductivity, refraction index, and extinction coefficients have been discussed in the pure and impure cases.

**Keywords:** InAs; Graphene-like; Fe impurity; Electronic properties; Magnetic properties; Optical properties

## 1. Introduction

Since conductor-based devices and semiconductors are crucial for modern technology, they become an intimate part of daily life. Although silicon is one of the best types of semiconductors due to its extensive applications [1], researchers are still looking for new high-quality materials with unique properties. In this regard, semiconductors of group III–V are suitable candidates and the elements of these groups have been used in designing optoelectronic devices due to their lattice parameters and energy gaps [2]. Indium arsenide with novel features like high electronic mobility, narrow bandgap, and light effective mass is one of the interesting compounds in this group.

Despite the significant properties of graphene, it cannot be used as a semiconductor because of its zero band gap, and the monolayers of other materials with nonzero energy have been used instead [3]. Although the structure of two-dimensional (2D) graphene-like materials is similar to graphene, their electronic and optical properties are different. The sheets such as MoSe<sub>2</sub> [4] and WSe<sub>2</sub> [5] have

unique applications in transistors, photodetectors, and electroluminescent devices due to their band gaps.

Recently, the tangible approaches about graphene motivated researchers to study 2D graphene-like materials [6–11] such as the 2D/quasi-2D nanocrystals of BN [6], MoS<sub>2</sub> [6], MoSe<sub>2</sub> [6], Bi<sub>2</sub>Te<sub>3</sub> [6], and Si [7]. Freeman et al. [9] utilized density functional theory (DFT) calculations on ultrathin films of BeO, AlN, SiC, GaN, ZnS, and ZnO and predicted the transformation of wurtzite (WZ) structures into a novel type of stable hexagonal BN-like structure. This prediction was then approved in other reports for ZnO [8, 12–14] and SiC [15–17].

Moreover, the stable structures of the monolayers of group III–V binary compounds were found by the first-principles calculations [3] where GaP was an indirect transition semiconductor and InP, GaAs, and InAs were direct transition semiconductors. Hence, the structures of these compounds made them applicable as a semiconductor in water splitting photocatalysts [3]. Sohrabi et al. [18] investigated the optical and electronic features of pure graphene-like InAs by density functional theory.

Graphene-like materials have considerable applications in food packaging, pollution absorption, shielding, flame-retardant, electronic devices, high-power electronics, drug delivery, biomedical treatment, and memory devices. Their

\*Corresponding author, E-mail: sohrabi1001@yahoo.com

unique mechanical and thermal properties, structural stability, and antioxidant ability motivated researchers to use them as fillers [19]. Adding graphene-like materials such as Bohr nitride to insulated thermoplastic polymers with low thermal conductivity improves their electrical properties and thermal conductivity [20]. Also, the mechanical properties of nano-composites improve by adding graphene-like materials [21]. Adding graphene-like materials to polymers increases their thermal stability which is demonstrated in several reports [22, 23]. Graphene-like materials such as polyvinylidene fluoride have the ability to separate organic pollution absorption, water and wastewater treatment, and contaminant elimination from oil [24, 25].

Doping pure graphene-like InAs with other elements has been carried out for different purposes and specific applications. Among doping elements, the transition metals attract a lot of attention in magnetic semiconductors, new spintronic industry, and magneto-optic devices.

In the present work, we studied the effect of Fe impurity on the electronic, magnetic, and optical features of graphene-like InAs using density functional theory and compared the results with the pure graphene-like. Regarding this novel synthesis method, we wish our predictions provide additional guidance for experimental approaches.

## 2. Computational method

The full-potential linearized augmented plane wave (FP-LAPW) method was performed within the density functional theory (DFT) framework as applied in the Wien2k package [26, 27]. Within our calculation, we chose  $R_{\text{Kmax}} = 9$  for pure graphene-like InAs and  $R_{\text{Kmax}} = 8.5$  for the case in which Fe impurity was added to InAs graphene-like.

$R_{\text{MT}}$  was the radius of the smallest muffin tin sphere, and  $K_{\text{MAX}}$  was the cutoff energy for a plane wave in the first Brillouin zone where the  $K$  point number was considered to be 1000 and 4000 for the electronic and optical calculations in pure graphene-like InAs, respectively. When the impurity was added to InAs graphene-like, the  $K$  point number was set as 300 and 800 for the electronic and optical calculations, respectively.

Moreover, in 2D-InAs, the radius of muffin tin spheres for As and In was 2 and 2.2, respectively. The separation energies for the pure and impure cases were  $-8$  Ry and  $-7$  Ry, respectively.

Here, the value of  $G_{\text{max}}$  which generated the largest vector in the Fourier expansion of charge density was considered as 14. GGA approximation was used for exchange–correlation potential, and the convergence of charge was 0.0001. It means that if the integration of input

and output charge density was less than 0.0001 among consecutive cycles, the cycles would stop. A hexagonal lattice structure with the P3m1 spatial group was observed in the graphene-like samples. The crystal structures of both pure and Fe-doped graphene-like InAs are shown in Fig. 1.

## 3. Results and discussion

### 3.1. Structural properties

In this section, the lattice constant of graphene-like InAs is calculated by considering the energy–volume diagram and its minimum point in Fig. 2 [18].

The supercell is used to investigate the structural features of graphene-like InAs with impurity. The bigger cell contains a certain number of the pure compound's cells which depends on the structure of pure compound and the number of the atoms. Here, an In atom is replaced by a Fe atom using the substitution method.

Adding Fe impurity caused the InAs bond length to decrease from 2.7045 to 2.5835 Å where the Fe-As bond length was 2.3088 Å. The angles of As-Fe-As, In-As-Fe, and As-In-As were  $116.403^\circ$ ,  $120.616^\circ$ , and  $112.986^\circ$ , respectively. These results were achieved from Xcrysden software.

### 3.2. Electronic properties

The density of states (DOS) and band structure have been used to study the electronic properties of crystals. The DOS diagrams were achieved by PBE-GGA approximation. As shown in Fig. 3, the compound has a semiconducting behavior and there is no state equal to the energy gap in the range of 0eV–0.92 eV [18].

As shown in Fig. 4, the DOS in up and down states did not coincide which is more obvious around the Fermi level at the range of 1 eV to  $-1$  eV. Hence, magnetic properties are expected for this compound. In fact, our calculations show that adding Fe impurity creates a total spin magnetic moment with the approximate value of  $5.00166 \mu_{\text{B}}$ . Therefore, Fe-doped graphene-like InAs with ideal magnetic properties can be used in magneto-optical devices. According to Fig. 4(a), there is no state equal to the energy gap in the range of 0.08–0.84 eV in the up spin and in the range of  $-0.47$  to 0.25 eV in the down spin (on an interval of about 0.72 eV). The most contribution of Fe atom in up and down spin is observed in the energy range of  $-2$  to  $-4$  eV and 0.5–1.5 eV, respectively. Furthermore, the lack of the DOS in down spin and the existence of DOS in up spin at the Fermi level of Fe-doped graphene-like InAs are clearly shown in Fig. 4(b). The presence of states is due to the presence of Fe impurity. According to the density of

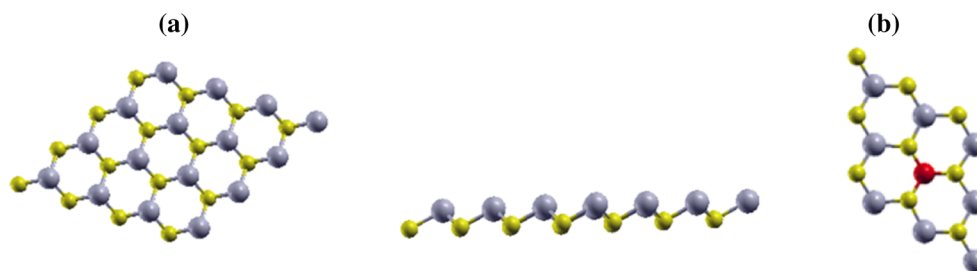


**Fig. 1** Side views and top views of (a) the pure graphene-like InAs and (b) graphene-like InAs doped with Fe atom. The yellow, blue, and red balls denote the atomic species of As, In, and Fe, respectively [18]

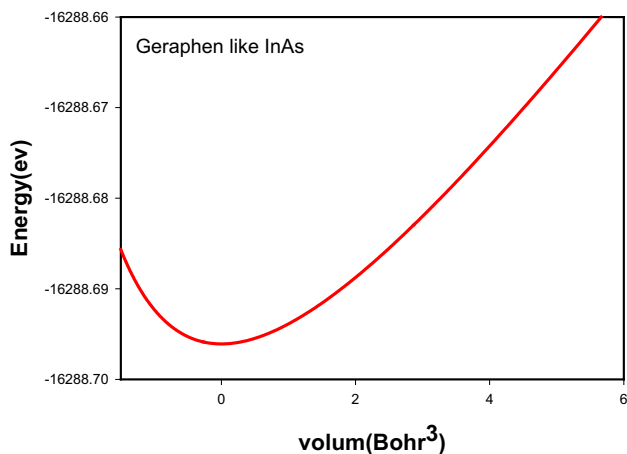


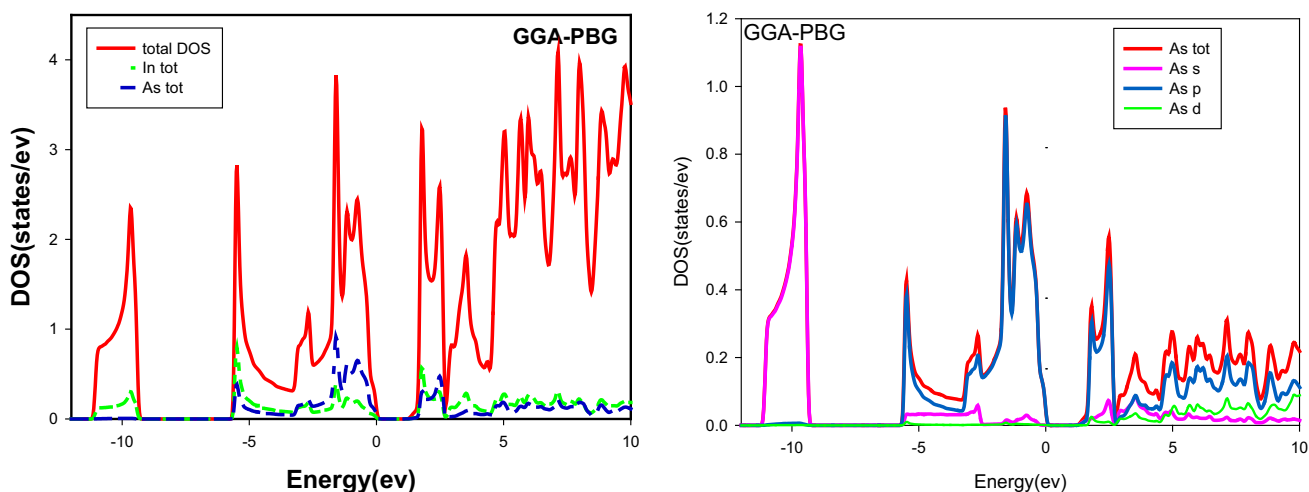
**Fig. 2** Diagram of total energy in terms of primitive cell volume for graphene-like InAs [18]

states, one can conclude that the Fe-doped graphene-like InAs is a half-metal with significant applications in spintronic devices because of its spin polarization and high magnetic moment. It should be noted that the spin polarization in the density of states comes from the hybridization between As-4p and Fe-3d orbitals.

Moreover, Figs. 5 And 6 represent the band structure of pure and Fe-doped graphene-like InAs, respectively, based on wave vectors, direction, and high symmetry points in the first Brillouin zone utilizing PBE-GGA approximation. In the pure graphene-like InAs, the band structure for up and down spins is the same. Also, the energy gap along  $K$  and  $\Gamma$  is direct—according to our results—and equal to 1.90972 and 0.92500 eV, respectively, which is in good agreement with other theoretical reports [18].

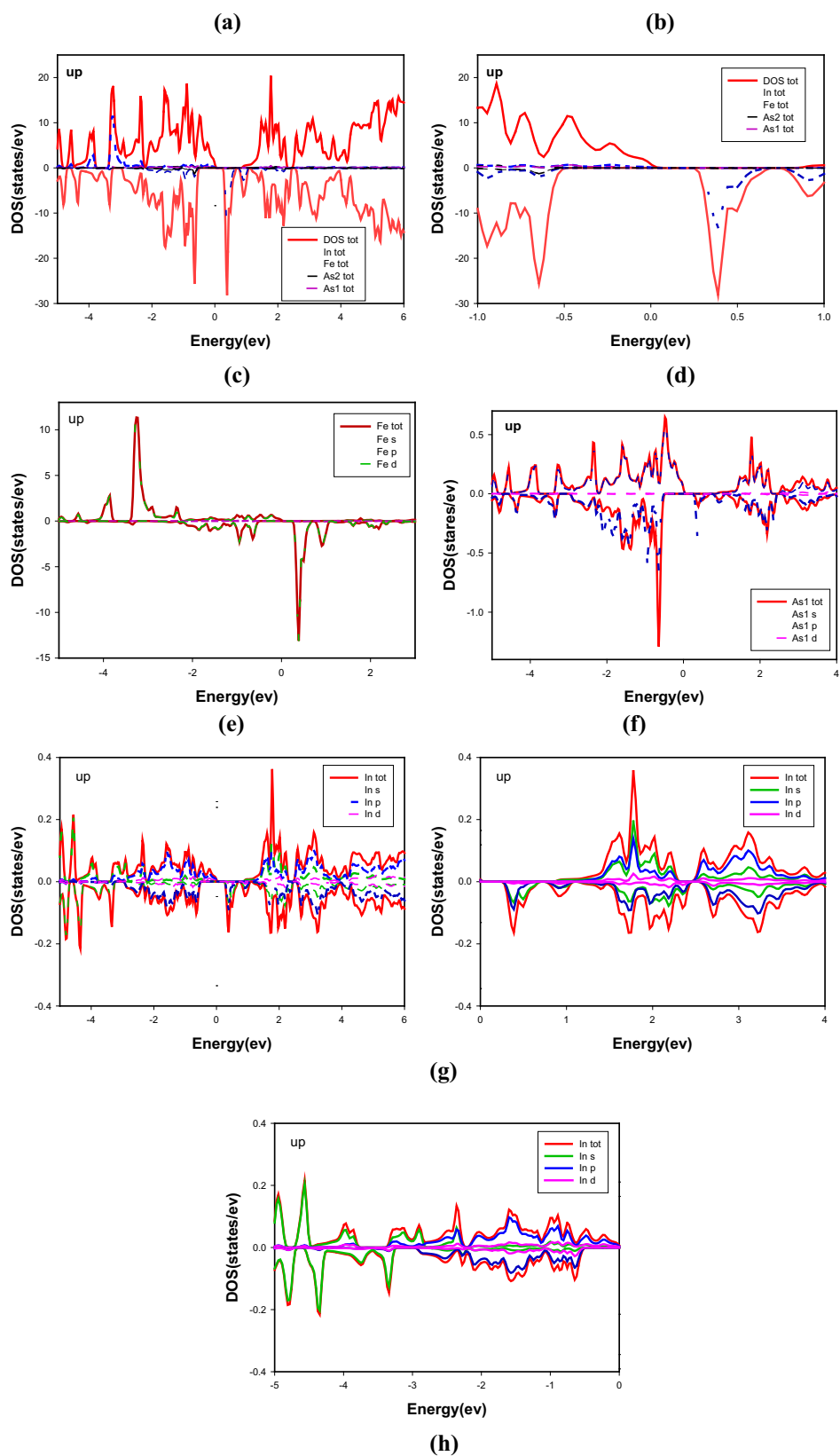
As shown in Fig. 6(a), the band structures in up and down spins do not coincide replacing Fe atoms and they differ with each other, especially near the Fermi level where most bands belong to Fe impurity. Besides, the mismatch of the diagrams represents magnetic properties. In the up spin, a direct gap of about 0.6 eV is observed along  $\Gamma$  direction, while in the down spin, a direct gap of about 0.85 eV is shown along  $\Gamma$  direction. The results confirm that replacing Fe impurity decreases energy gap and the increases the number of bands. The existence of bands below Fermi level at the range of 0 to  $-5.5$  eV (diagram (b)) and  $-0.45$  to  $-2.5$  eV (on diagram (a)) is mainly due to d orbitals of Fe impurity.

In Fig. 6(a) and (b), most lines along  $\Gamma$ -A direction are flat because the speed of electrons is low and their effective



**Fig. 3** Diagram of partial and the total DOS of graphene-like InAs obtained within the PBE-GGA [18]

**Fig. 4** Diagrams of (a) total density of states for graphene-like InAs with the influence of In, As and Fe atoms, (b) total density of states in the range of 1 eV to  $-1$  eV for graphene-like InAs doped by Fe, partial density of states for (c) Fe, (d) As, and (e) In, and density of states in (f) above the Fermi level and (g) below the Fermi level. (As1 and As2 denote As atoms close to and far from the Fe atom.)



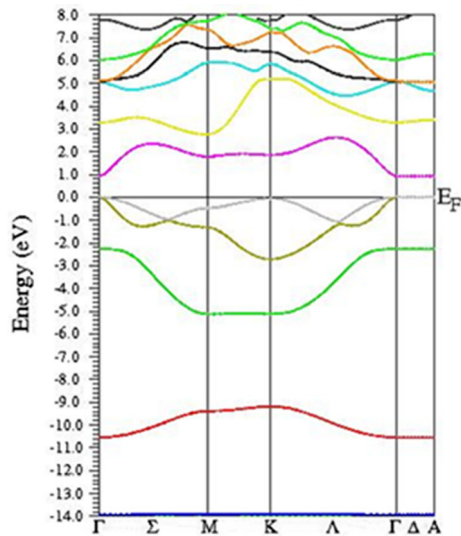


**Fig. 5** Band structure of the pure graphene-like InAs along the great symmetric points in the first Brillouin zone using PBE-GGA approximation [18]

mass is high in this direction which results in their less contribution in conductivity.

### 3.3. Optical properties

In order to study optical features, the diagrams of the imaginary and real parts of loss function, dielectric function, refraction index, extinction coefficient, and optical conductivity have been discussed in this section.

Here, the GGA-PBG technique is applied to assess optical properties. Figure 7 depicts the changes in the real part of dielectric function versus incident photon energy. The static value, the peaks, and the roots of the real part of dielectric function are listed in Table 1 based on the relation  $n(0) = \sqrt{\varepsilon_1(0)}$ . Although adding impurity increases the static dielectric function along the x-axis, no change is observed in the z-axis.

As the energy of the incident photon increases to about 13.5 eV, the real part of dielectric functions along x and z directions becomes nearly coincident in both diagrams. By comparing the static dielectric function, the peaks, and the roots of the real part of dielectric function in  $Ell_z$  of both diagrams, it is obvious that adding Fe impurity to graphene-like InAs causes no sensible change in this direction.

Figure 8(a) and (b) shows the imaginary part of the dielectric function when the electric field with different energies is applied parallel and perpendicular to the surface of the pure and Fe-doped graphene-like InAs. As shown in Fig. 8(a), the imaginary part of dielectric function for the pure graphene-like InAs is too small for energies less than 0.7 eV and 1.92 eV for  $Ell_x$  and  $Ell_z$ , respectively. On the other hand, Fig. 8(b) shows that in like graphene InAs doped with Fe, this imaginary part is too small for energies less than 0.5 eV and 0.89 eV in  $Ell_x$  and  $Ell_z$ , respectively. Moreover, the highest peak in Fig. 8(a) for  $Ell_x$  at 2.28 eV is related to the optical transition from As-4p to In-5s, and hence, the majority of absorption happens in the visible region. For  $Ell_z$ , the highest peak of  $\varepsilon_2(\omega)$  is about 6.96 eV.

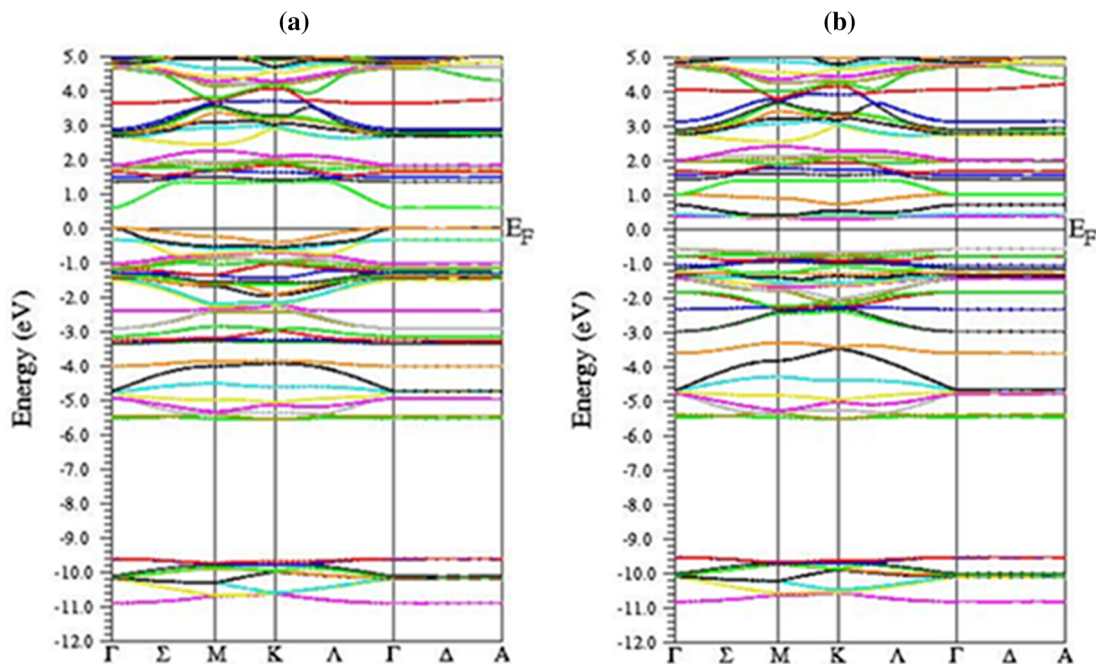


**Fig. 6** Band structure in InAs graphene-like by replacing Fe impurity (a) in up spin mode and (b) in down spin mode

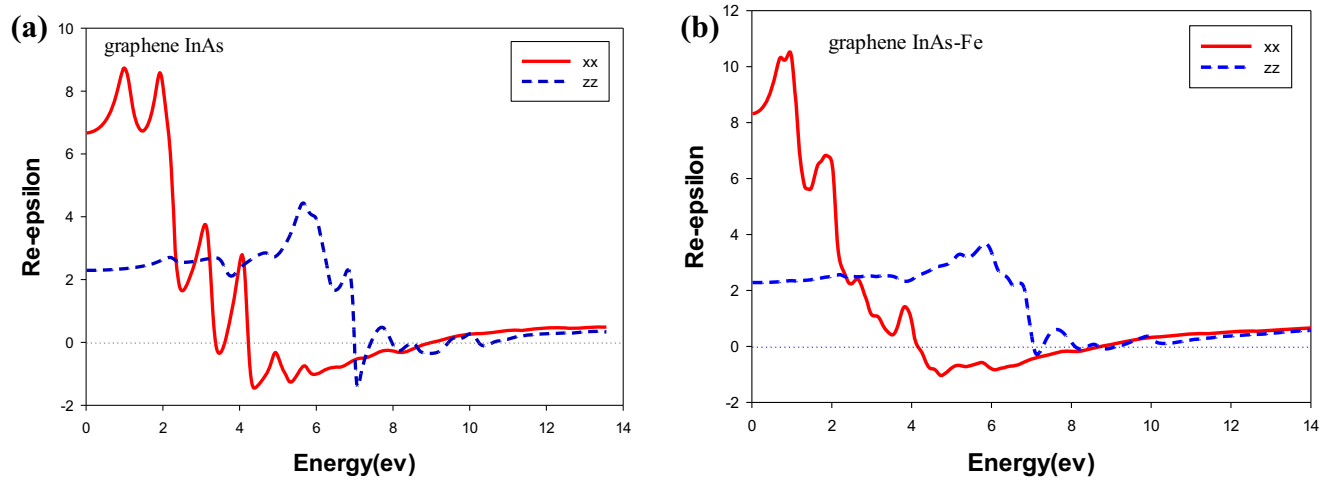


**Fig. 7** Changes of the real part of dielectric function in  $Ell_x$  and  $Ell_z$  for (a) the pure graphene-like InAs [18] and (b) graphene-like InAs doped by Fe

**Table 1** Dielectric constant, static refraction index, and the roots of the real part of dielectric function in pure graphene-like InAs and the graphene-like InAs doped by Fe atom in terms of incident energy for  $Ell_x$  and  $Ell_z$

	InAs graphene-like	InAs graphene-like + Fe
$\epsilon_0_x$	6.69	8.26
$n_0_x$	2.59	2.87
$\epsilon_0_z$	2.3	2.3
$n_0_z$	1.51	1.51
The peak energy (eV) along $x$	1.00	0.95
The peak of the energy (eV) along $z$	5.69	5.82
The root of the real part of dielectric function along $x$	3.37–3.63–4.23–8.97	4.07–8.78
The root of the real part of dielectric function along $z$	9.5–8.5–7.94–7.40–6.69	9.18–8.65–8.46–8.04–7.32–7.01

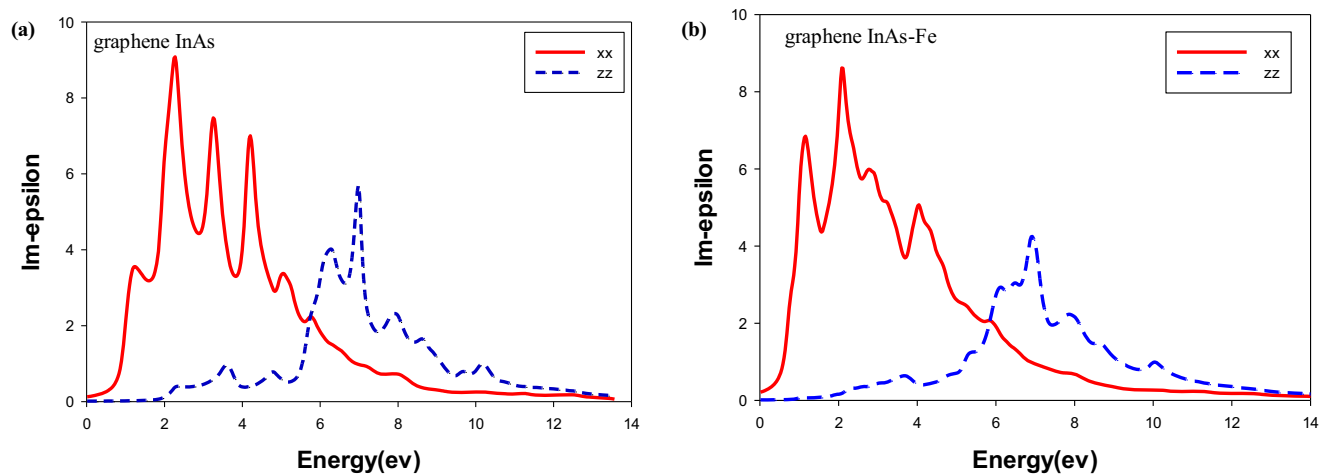


**Fig. 8** Changes of the imaginary part of dielectric function for  $Ell_x$  and  $Ell_z$  in (a) pure graphene-like InAs [18] and (b) graphene-like InAs doped with Fe



As shown in Fig. 8(b), adding Fe impurity to graphene-like InAs creates the highest peaks as about 2.01 eV along x-axis and 6.92 eV along z-axis which is due to the optical transition from Fe-3d to As-4p. Since most of the peaks along x-axis are located at the energies from 1 to 5 eV in both diagrams, it is expected that the highest absorption occurs in the visible and even ultraviolet regions. Along z-axis, however, most of the peaks are observed at the energies about 7 eV which means that the highest absorption in this direction occurs in the ultraviolet region.

It can be demonstrated that by replacing In with Fe in InAs graphene-like, the number of peaks and the intensity of  $\varepsilon_2(\omega)$  decrease in both directions and the peaks of the imaginary part of dielectric function shift toward lower energies.

Figure 9 shows the diagram of the energy loss function of the electron in terms of the energy of incident photon. By comparing the energy gap found in the previous section and the result of Fig. 9(a), it is obvious that there are no considerable changes in the energy loss function for energies less than 0.98 eV and 1.96 eV along x-axis and z-axis, respectively. In Fig. 9(b), also, there is not any significant change in the energy loss function for the energies less than 0.6 eV and 1 eV along x-axis and z-axis, respectively.

It should be noticed that the energy of plasmonic oscillations is about 9 eV in both diagrams and the energy loss function in x-direction is higher than that in z-direction in both diagrams. When the impurity is injected into graphene-like InAs, the plasmonic energy moves slightly toward lower energies in both directions.

Furthermore, refractive index is one of the most important parameters that should be considered in optical applications and designs. Recently, the requirement for materials with high refractive index has been increased in medical filters, lenses, optical adhesives, antireflection

coatings, and enhanced optoelectronic components [28–35].

Figure 10(a)–(c) shows the variation in the refractive index in terms of the energy of the incident photon along the x-axis and z-axis. As can be seen, the graphs of the pure and Fe-doped graphene-like InAs are similar to the real part of the dielectric function.

In addition, the identical value of static refractive index (= 1.51) in z-direction for pure and Fe-doped graphene-like InAs is indicated in Fig. 10(a) and (b). Thus, adding impurities does not affect the static index of the compound in this direction. The values obtained from the graph are in good agreement with the results of the real part of dielectric function as  $n(0) = \sqrt{\varepsilon_1(0)}$  in Table 1.

From Fig. 10, the maximum refractive index of graphene-like InAs along z-axis is 2.14 at the energy of 5.67 eV. By replacing Fe impurity, it reaches 1.98 at the energy around 5.92 eV which means that by adding Fe impurity, the maximum refractive index is decreased in higher energies.

The refractive index in graphene-like InAs is less than the unity along z-axis at energies more than 8eV where the superluminal behavior is observed. Comparing pure graphene-like InAs, adding Fe impurity causes no sensible changes in the threshold of superluminal wave. The superluminal effect typically refers to the phenomena where the speed of electromagnetic waves is higher than the speed of light in vacuum.

On the other hand, the value of static refractive index along the x-axis in pure and Fe-doped graphene-like InAs is 2.59 and 2.89, respectively, which shows the increase in static refractive index by adding Fe. These values achieved from the graph are well matched with the calculated values of the real part of the dielectric function in the former section. Moreover, the value of static refractive index is

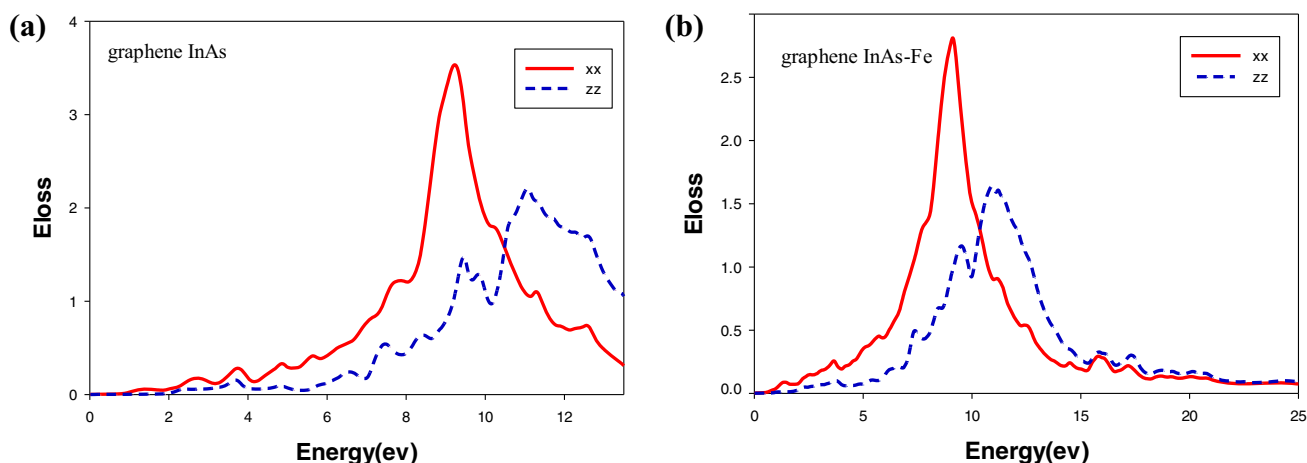


**Fig. 9** Diagram of energy loss function versus the incident photon energy for  $E_{lx}$  and  $E_{lz}$  in (a) pure graphene-like InAs [18] and (b) graphene-like InAs doped with Fe

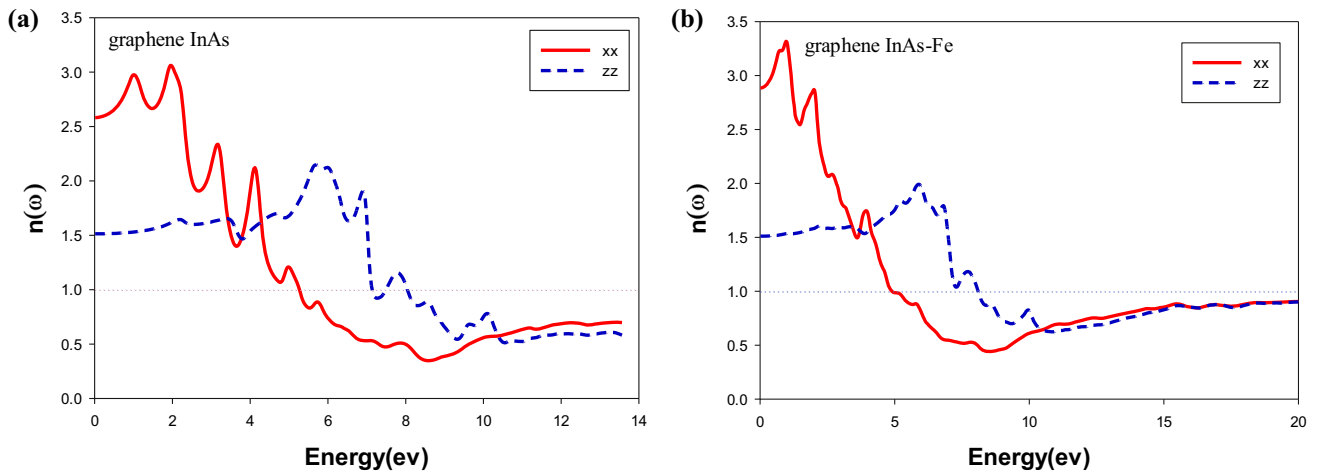


**Fig. 10** Diagram of the refractive index versus the energy of incident photon in both x- and z- directions for (a) graphene-like InAs [18] and (b) graphene-like InAs doped with Fe atom

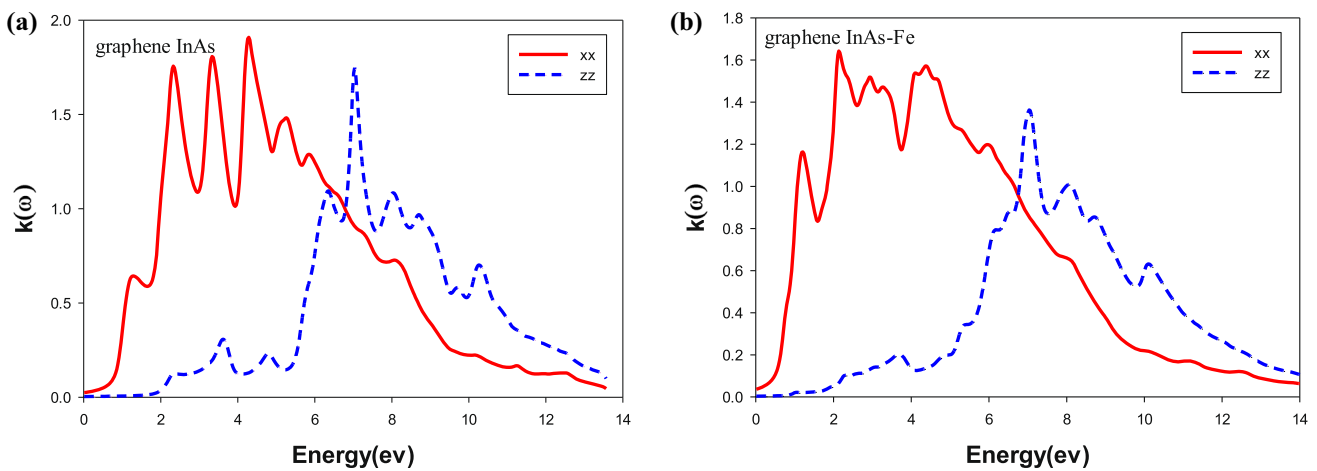


**Fig. 11** Diagram of the extinction coefficient versus the energy of incident photon in both x- and z- directions for (a) graphene-like InAs [18] and (b) graphene-like InAs doped with Fe atom

comparable to that in silicon and germanium (two common elements used in solar cells) which are 3.42 and 4.06, respectively [36]. The large value of refractive index in graphene-like InAs along x-axis improves its application in photonic while the magnetic properties of the Fe-doped graphene-like InAs make them useful in magneto-optical devices.

The maximum value of the refractive index along x-axis in graphene-like InAs is 2.01 at the energy 3.07 eV, and by adding Fe impurity, it reaches 3.31 at the energy around 0.97 eV which confirms the increase in maximum refractive index by adding Fe impurity. Along the x-axis, the refractive index of graphene-like InAs for the energies more than 5.27 eV is less than unity and the superluminal behavior is observed. Adding Fe impurity creates the

threshold of the superluminal wave in the energies more than 4.86 eV.

Accordingly, the maximum value of refractive index along x-axis for both pure and doped graphene-like InAs is located in the visible and even ultraviolet regions. However, along z-axis, the maximum refractive index is located in the ultraviolet region for both pure and Fe-doped graphene-like InAs.

Figure 11(a) and (b) shows the variation in the extinction coefficient in terms of incident photon energy along x-axis and z-axis. As can be seen, the highest peaks of extinction coefficient along x-axis for pure graphene-like InAs and graphene-like InAs doped with Fe atom exist at about 4.80 eV and 2.16 eV, respectively. Similarly, the maximum peaks of their extinction coefficient along z-axis



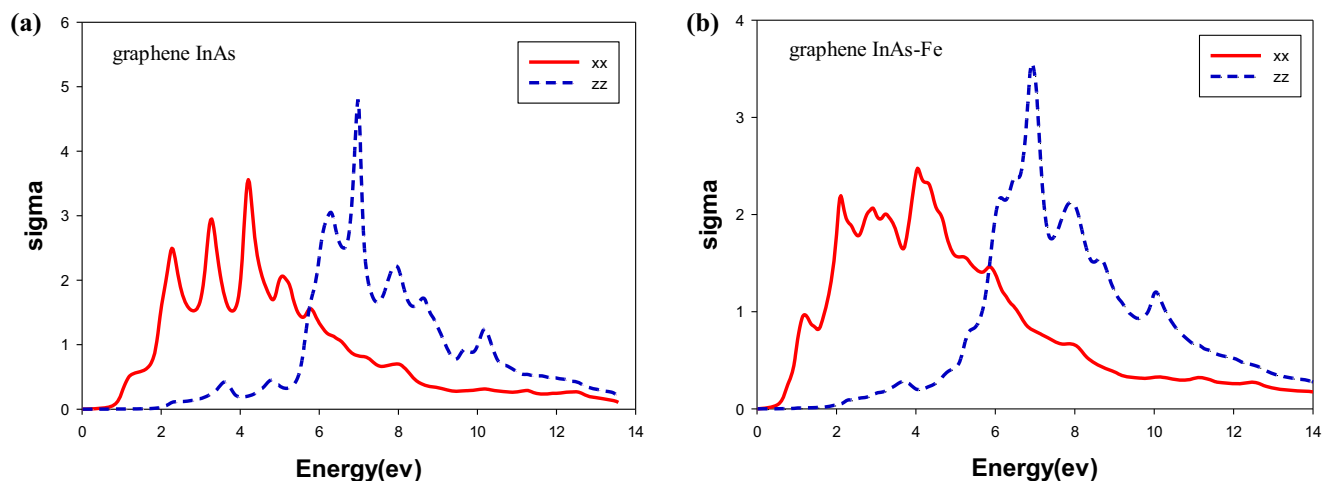


**Fig. 12** Real part of optical conductivity versus the energy of incident photon in both x- and z- directions for (a) graphene-like InAs [18] and (b) graphene-like InAs doped with Fe atom

occur at about 7.17 eV and 7.08 eV, respectively. These results are matched well with the roots of the real part of the dielectric function. Besides, the highest peak of the extinction coefficient along x-axis in pure graphene-like InAs is higher compared to Fe-doped graphene-like InAs.

Moreover, the diagram of Fig. 12 for pure graphene-like InAs revealed that there is no conductivity along x- and z-axis in energies less than 0.80 eV and 2 eV, respectively. In graphene-like InAs with Fe impurity, however, the conductivity is zero along x-axis and z-axis for energies less than 0.53 and 0.8 eV, respectively, which are equal to the values of the energy gaps. The peaks are related to the transitions of electrons from the filled state under the Fermi level to the unfilled states in the conduction band which are in good agreement with the transitions achieved through the imaginary part of the dielectric function. This conductivity is rapidly reduced after 14 eV in both cases.

#### 4. Conclusions

In this work, the optical and electronic properties of pure graphene-like InAs and graphene-like InAs doped with Fe impurity were investigated in terms of density functional theory by GGA-PBE approximation and the results were compared. The values of the angle within the adjacent bonds ( $\theta$ ), the nearest adjacent distance ( $d$ ), and the minimum value of the energy gap ( $E_g$ ) were determined for the pure graphene-like InAs and the graphene-like InAs in the presence of Fe impurity. By studying the electronic properties and GGA-PBE approximation, it was found that these compounds had direct gaps at the  $\Gamma$  and  $K$  points with

the values of 0.92500 eV and 1.90972 eV, respectively. Moreover, the graph of the band structure in the up and down spin did not coincide in the Fe-doped case which indicated its magnetic properties. The total magnetic moment of about 5.00166 Bohr Magnetron in our calculations confirmed high magnetic properties. In addition, the Fe-doped graphene-like InAs had direct gap along  $\Gamma$  in the up-spin and down-spin at around 0.6 eV and 0.85 eV, respectively. Based on the lack of DOS in the down-spin and the presence of DOS in the up-spin, it was suggested that the graphene-like InAs doped with Fe impurity is a magnetic semiconductor.

In addition, studying optical properties revealed the static dielectric function as  $\epsilon_{1x}(0)=6.69$  and 8.26, and  $\epsilon_{1z}(0)=2.3$  and 2.3 for the pure and Fe-doped graphene-like InAs, respectively.

Besides, the threshold energy in the optical diagrams matched well with the energy gap achieved from the DOS diagrams and band structure. The static refractive index was  $n_{xx}(0)=2.26$  and 2.89 in pure and Fe-doped graphene-like InAs, respectively. Along the z-axis, however, refractive index was 1.51 for both samples.

Moreover, the diagram of Eloss indicated that the plasmonic frequency was relative to the real part of dielectric function and its value for graphene-like InAs and Fe-doped graphene-like InAs was found 9 eV and 8 eV in x-direction and 11 eV and 10 eV in z-direction, respectively. Finally, for pure graphene-like InAs, the maximum conductivity achieved in the radiation around 5 eV in x-direction and in the ultraviolet radiation around 7 eV in z-direction. The redshift appeared in the optical coefficients by adding Fe impurity to the graphene-like InAs.

## References

- [1] M I Ziane, Z Bensaad, B Labdelli and H Bennacer *Sensors & Transducers*. **27** 374 (2014)
- [2] N Bouarissa and R Bachiri *Phys. B*. **322** 193 (2002)
- [3] T Suzuki *Appl. Phys. Lett* **107** 213105 (2015)
- [4] I Ahmad, S A Khan, M Idrees, M Haneef, I Shahid, H U Din, S A Khan and B *Physica B*. **545** 113 (2018)
- [5] D Muoi, N N Hieu, H T Phung, H V Phuc, B Amin, B D Hoi, N V Hieu, L C Nhan, C V Nguyen, P T T Le *Chem. Phys.* **519** 69 73 (2019).
- [6] A H C Neto and K Novoselov *Rep. Prog. Phys* **74** 1 (2011)
- [7] A Kara, H Enriquez and et al. *Surf. Sci. Rep.* **67** 1 (2012)
- [8] C Tusche and et al. *Phys. Rev. Lett.* **99** 026102 (2007)
- [9] C L Freeman and et al. *Rev. Lett.* **96** 066102 (2006)
- [10] H Sahin, S Cahangirov, M Topsakal, E Bekaroglu, E Akturk, R T Senger and S Ciraci *Phys. Rev. B*. **80** 155453 (2009)
- [11] S Wang *J. Phys. Soc. Jpn.* **79** 064602 (2010)
- [12] L I Alexander *Russ. Chem. Rev* **81** 571 (2012)
- [13] X Y Feng, Z Wang, C W Zhang, P J Wang *Phys. E: Low Dimens. Syst. Nanostruct* **54** 144 (2013)
- [14] G Mukhopadhyay, H Behera *World J. Eng* **10** 39 (2013)
- [15] S S Lin *J. Phys. Chem. C* **116** 3951 (2012)
- [16] N S Eliseeva, A A Kuzubov, S G Ovchinnikov, M V Serzhan-tova, F N Tomilin, A S Fedorov, *JETP Lett* **95** 555 (2012)
- [17] X Lin, S Lin, Y Xu, A A Hakro, T Hasan, B Zhang, B Yu, J Luo, E Li, H Chen *J. Mater. Chem. C* **1** 2131 (2013)
- [18] L Sohrabi, A Boochani, S A Sebt and M Elahi *Eur. Phys. J. Plus* **133** 117 (2018)
- [19] C Yu, J Zhang, W Tian, X Fan, Y Yao. *ACS Appl. Mater. Interfaces* (2018). <https://doi.org/10.1021/acsami.5b03007>
- [20] V. Guerra, C. Wan, T. McNally. (2019). <https://doi.org/10.1021/jp0607014>
- [21] H.L. Nguyen, Z. Hanif, S.A. Park, B.G. Choi, T.H. Tran, D.S. Hwang, et al. (2018). <https://doi.org/10.3390/polym.10050.501>
- [22] K. Wenelska, K. Maslana, E. Mijowska. (2018). <https://doi.org/10.1039/C8RA01527A>
- [23] YK. Shin, WS. Lee, MJ. Yoo, ES. Kim. (2013). <https://doi.org/10.1016/j.ceramint.2012.10.137>
- [24] R. Moradi, M. Shariaty-Niassar, N. Pourkhalili, M. Mehrizade, H. Niknafas. (2018). <https://doi.org/10.12989/MWT.2018.9.4.221>
- [25] A.R. Kamble, C.M. Patel, Z.V.P. Murthy. (2018). <https://doi.org/10.1080/01496395.2018.1496118>
- [26] P Blaha, K Schwarz, P Sorantin and S B Trickey *Comput. Phys. Commun.* **59** 399 (1990)
- [27] K Schwarz, P Blaha *Comput. Mater. Sci.* **28** 259 (2003)
- [28] Z Cui, C LCU, B Yang, J.Shen and et al. *polymer* **42** 10095 (2001)
- [29] R Okutsu, S Ando and M Ueda *Chem. Mater* **20** 4017 (2008)
- [30] A Nebioglu, J A Leon and I V Khudyakov *Ind. Eng. Chem. Res.* **47** 2155 (2008)
- [31] S D Hart, G R Maskaly, ranTemelku and p B H prideaux et al. *Science*. **296** 510 (2002)
- [32] J A Dobrowolski and F Ho *Appl.Opt.* **21** 288 (1982)
- [33] E Yablonovitch *Science* **289** 557 (2000)
- [34] L A Hornak *polymers for light wave and Integrated Optics Technology and Applications*, (Marcel Dekker: New York) (1992)
- [35] A H Kitai *Solid state Luminescence*, (Chapman Hall. London) (1993)
- [36] H H Li *J. Phys. Chem. Ref. Data.* **9** 561 (1980)

**Publisher's Note** Springer Nature remains neutral with regard to jurisdictional claims in published maps and institutional affiliations.